Journal of Alloys and Compounds 509 (2011) L34–L37

Contents lists available at ScienceDirect

Journal of Alloys and Compounds

journal homepage: www.elsevier.com/locate/jallcom

Letter

Direct transformation from goethite to magnetite nanoparticles by mechanochemical reduction

Tomohiro Iwasaki [a,*], Nami Sato [a], Kazunori Kosaka [a], Satoru Watano [a], Takeshi Yanagida [b], Tomoji Kawai [b]

[a] Department of Chemical Engineering, Osaka Prefecture University, 1-1 Gakuen-cho, Nakaku, Sakai, Osaka 599-8531, Japan
[b] Institute of Scientific and Industrial Research, Osaka University, Osaka 567-0047, Japan

ARTICLE INFO

Article history:
Received 4 August 2010
Received in revised form 6 October 2010
Accepted 7 October 2010
Available online 16 October 2010

Keywords:
Magnetic materials
Magnetite nanoparticles
Goethite
Mechanochemical reduction
Ball-milling
Magnetic properties

ABSTRACT

We present a novel method for synthesizing highly crystalline superparamagnetic magnetite (Fe_3O_4) nanoparticles (particle size about 15 nm) with relatively high saturation magnetization by direct transformation via ball-milling treatment from an amorphous goethite precipitate in a water system at room temperature. The obtained product was characterized by transmission electron microscopy, X-ray diffraction, and energy-dispersive X-ray spectroscopy; the particle size was measured by dynamic light scattering particle size analysis, and magnetic properties were measured by superconducting quantum interference device magnetometer. The mechanochemical effect induced by ball-milling treatment generates hydrogen gas, which contributes in reduction of part of the goethite, without addition of reducing agents, to give ferrous hydroxide. The mechanochemical effect also promotes solid-phase reaction between ferrous hydroxide and goethite to give magnetite, simultaneously crystallizing the formed magnetite nanoparticles while inhibiting particle growth with addition of neither heat nor additives such as surfactants and organic solvents. Thus, mechanochemical reduction provides an easy route for the synthesis of crystalline magnetite nanoparticles from ferric ion solution.

1. Introduction

Among magnetic materials, magnetite (Fe_3O_4) is particularly important. Fe_3O_4 nanocrystal powder has excellent magnetic properties and is nontoxic, highly stabile, and promising for biological applications such as immobilization of enzymes [1–3] and proteins [4–6], magnetic separation of cells [7–9], and synthesis of a nucleotide [10]. Superparamagnetic Fe_3O_4 nanoparticles are important for biomedical applications such as drug delivery [11–14], magnetic resonance imaging [15–18], hyperthermia [19–21], and immunoassays [22–24].

Various methods have been developed for the synthesis of superparamagnetic Fe_3O_4 nanoparticles in gas, liquid, and solid phases. Liquid-phase synthesis methods such as coprecipitation that use iron hydroxide precursor are practical on an industrial scale because the chemical reactions are relatively easy to control [25–30]. However, conventional synthesis methods have several problems, including high levels of complexity and requirement for reagents that are incompatible with or toxic to the human body [31,32]. Non-conventional green synthesis methods have also been proposed [33–35]. For example, Lu et al. [35] used glucose as a nontoxic reducing agent, and used gluconic acid, which is the oxidative product of glucose, as a stabilizer and dispersant. In such methods, however, reactions are still carried out under environmentally unfriendly conditions, such as high temperature or high pH.

To help devise a more environmentally friendly method for industrial production, we have proposed a simple mechanochemical synthesis method by which superparamagnetic Fe_3O_4 nanoparticles are prepared by ball-milling a neutral precursor suspension of ferrous hydroxide and goethite (α-FeOOH) at room temperature in a water system [36]. The obtained results suggested that ferric ions were reduced in the milling treatment although no reducing agent was used. In this paper, for simplifying the synthesis process, a synthesis method in which α-FeOOH is directly transformed to Fe_3O_4 by means of the mechanochemical reduction effect has been developed, and the reaction mechanism is discussed.

2. Experimental

All chemicals used in the experiments were of analytical reagent grade and were used without further purification. The total iron concentration in the initial solution was the same as for our previous studies [36–38]. 4.5 mmol of ferric chloride hexahydrate ($FeCl_3 \cdot 6H_2O$) was dissolved in 60 ml of deionized and deoxygenated water in a beaker. 13.5 mmol of sodium hydroxide (NaOH) was added to the solution by dropping a proper amount of 1.0 kmol/m^3 NaOH solution at room temperature under vigorous stirring by magnetic stirrer in an argon atmosphere. The pH of the

* Corresponding author. Tel.: +81 72 254 9307; fax: +81 72 254 9911.
E-mail address: iwasaki@chemeng.osakafu-u.ac.jp (T. Iwasaki).

0925-8388/$ – see front matter © 2010 Elsevier B.V. All rights reserved.
doi:10.1016/j.jallcom.2010.10.029

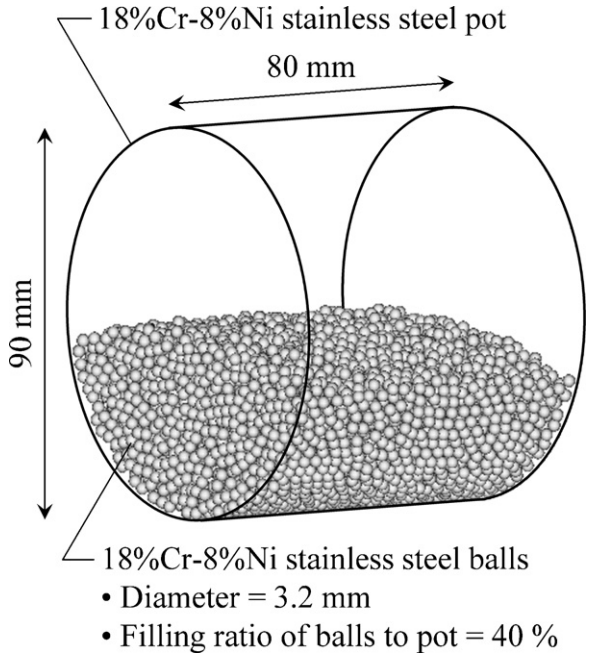

Fig. 1. Schematic of tumbling ball mill used in this work.

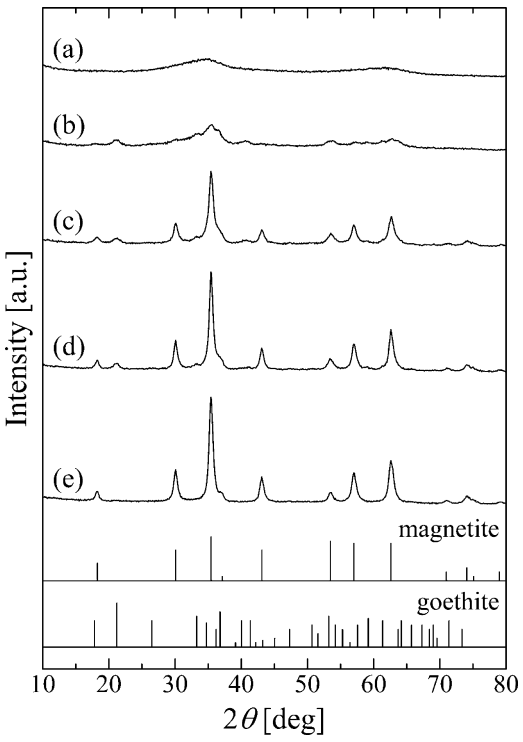

Fig. 2. XRD patterns of samples (a) before and after ball-milling treatment for (b) 1 h, (c) 2.5 h, (d) 4 h, and (e) 7 h. The vertical bars at the bottom represent the standard diffraction data for magnetite (ASTM card #11-614) and goethite (ASTM card #3-249).

solution was 8.3. The addition of NaOH gives α-FeOOH according to the following reactions:

$$Fe^{3+} + 3OH^- \rightarrow Fe(OH)_3 \quad (1)$$

$$Fe(OH)_3 \rightarrow \alpha\text{-FeOOH} + H_2O \quad (2)$$

The reddish-brown initial suspension thus prepared was poured into a milling pot (inner diameter 90 mm, capacity 500 ml) made of 18%Cr–8%Ni stainless steel. Stainless steel balls (diameter 3.2 mm) were used as the milling media; the charged volume of the balls (including voids among the balls) was 40% of the pot capacity, as illustrated in Fig. 1. The milling pot was purged of air, filled with argon, and sealed. The ball-milling treatment was performed at room temperature for a designated period of time by rotating the milling pot. The rotational speed was 140 rpm, which corresponds to 64% of the critical rotational speed of 220 rpm (determined experimentally depending on the actual motion of balls involving the starting suspension). After the treatment, the suspension temperature had risen by 3–4 °C. The obtained precipitate was washed with deionized water, centrifuged (centrifugal acceleration 1500 × *g*), and decanted. After this washing operation was repeated three times, the precipitate was dried overnight at 30 °C under vacuum.

The morphology of the sample was observed by field emission transmission electron microscopy (TEM; JEM-2100F, JEOL). The chemical composition was determined by energy-dispersive X-ray spectrometry (EDS; JED-2300F, JEOL). The iron content was determined by oxidation–reduction titration [39]. The hydrodynamic size was measured by dynamic light scattering (DLS; DLS-7000, Otsuka Electronics) for a sample-redispersed aqueous suspension after ultrasonic irradiation. The median diameter (number basis) was determined from the obtained size distribution. The powder X-ray diffraction (XRD) pattern was obtained by X-ray diffractometer (RINT-1500, Rigaku; Cu Kα radiation, $2\theta = 10°–80°$, scanning rate 1.0°/min). The average crystallite size was calculated from the full width at half-maximum (FWHM) of the Fe_3O_4 (3 1 1) diffraction peak at $2\theta \approx 35.5°$ using Scherrer's formula. The lattice constant was determined from several diffraction angles showing high-intensity peaks. The magnetic properties (magnetization–magnetic-field hysteretic cycle) were analyzed by superconducting quantum interference device (SQUID) magnetometer (MPMS, Quantum Design) at room temperature in a magnetic field range of −10 to +10 kOe.

The mechanochemical effect on the synthesis of Fe_3O_4 was investigated by performing ball-milling treatment of $FeCl_3$ solution to which NaOH was not added at room temperature. The solution absorbance was measured at room temperature by spectrophotometer (Ubest V-530, JASCO). The composition of the gas phase in the milling pot after the treatment was qualitatively analyzed by gas chromatography (GC; CP-3800, Varian).

3. Results and discussion

Fig. 2 shows XRD patterns of samples before and after the ball-milling treatment. Before the treatment, the sample contained an amorphous phase of α-FeOOH. As the milling time elapsed, α-FeOOH crystallized and disappeared, and Fe_3O_4 crystallized simultaneously. By 7 h, single-phase Fe_3O_4 was formed and the pH of the suspension was 6.7. Peaks indicating the formation of other compounds and contamination caused by wear of the milling pot and balls were not observed.

EDS analysis, performed to detect small amounts of impurity, showed that the sample contains only small amounts of contaminants: just 1.52 wt% Cr, 0.84 wt% Ni, 0.13 wt% Na, and 0.04 wt% Cl. Impurity levels can be reduced even further by decreasing the rotational speed, although doing so may increase the milling time required to obtain single-phase Fe_3O_4 [38]. The sample had an atomic ratio of 43.8% Fe and 56.2% O, which was near the theoretical value for Fe_3O_4 (42.9% Fe and 57.1% O). Oxidation–reduction titration showed that the iron content was 72.6 wt%, which was also near the theoretical value for Fe_3O_4 (72.4 wt%). In addition, the lattice constant was 8.392 Å, which was very much nearer to the standard value for Fe_3O_4 (8.396 Å) than to the value for maghemite (γ-Fe_2O_3) (8.345 Å) or for Fe_3O_4 nanoparticles prepared by conventional coprecipitation methods (e.g., Ref. [28]). The lattice constant for the formed Fe_3O_4 phase remained almost constant regardless of the milling time. These results suggest that the sample consisted mostly of homogeneous single-phase Fe_3O_4.

Figs. 3 and 4 show typical TEM images and DLS particle-size distribution, respectively, for a sample prepared by ball-milling for 7 h The particle size was in the range 10–20 nm, almost in agreement with the average crystallite size (12.0 nm) calculated from the XRD pattern and the median diameter (17.1 nm) determined by DLS analysis. The HR-TEM image indicates that the nanoparticles have a single-crystal structure. Thus, it is confirmed that fine Fe_3O_4 nanoparticles of high crystallinity can be synthesized without addition of heat or reducing agents.

Fig. 5 shows the results of magnetization-magnetic field hysteresis. The sample exhibits ferromagnetic behavior with a relatively high saturation magnetization of 88 emu/g. Its coercivity

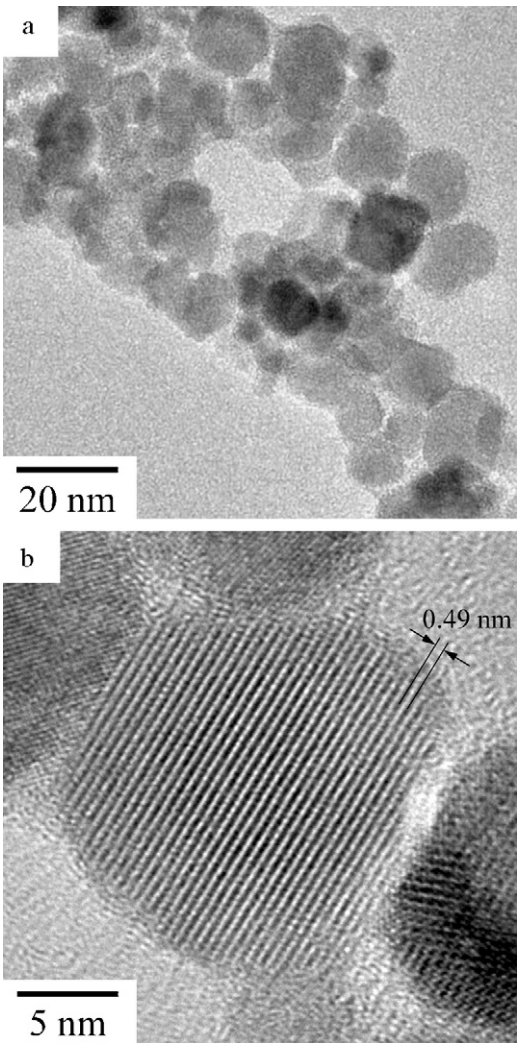

Fig. 3. (a) TEM and (b) HR-TEM images of sample obtained for 7 h.

is about 8 Oe, showing superparamagnetism. In contrast, well-crystallized bulk Fe_3O_4 has a saturation magnetization of 92 emu/g [40]. Saturation magnetization is known to be affected by the particle size, crystallinity, and contamination [41], and decreases with

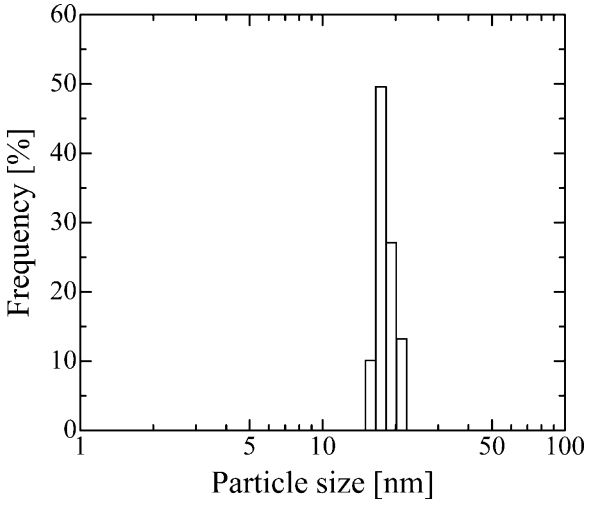

Fig. 4. Hydrodynamic particle size distribution of sample obtained for 7 h.

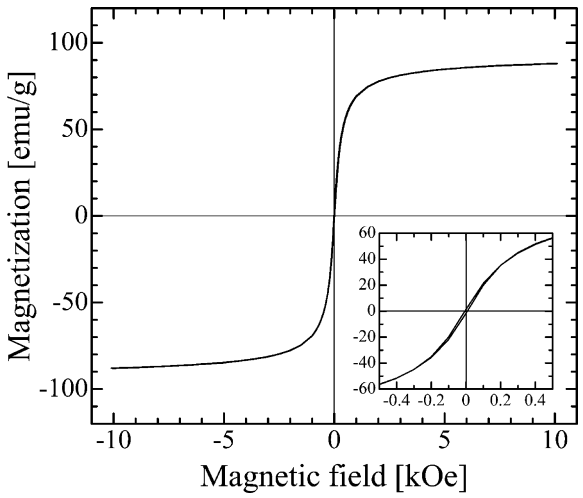

Fig. 5. Magnetic hysteresis loop of sample obtained for 7 h. The inset shows enlarged view of the central region of the loop.

decreasing particle size, low crystallinity, and the presence of impurities [42]. Although the sample's particle size is very small, its saturation magnetization was close to that of the bulk, indicating that it was well-crystallized and consisted of homogeneous single-phase Fe_3O_4.

Fig. 6 shows the UV spectra of ball-milled $FeCl_3$ and unmilled $FeCl_2$ solutions. As the milling time elapsed, the typical peaks at 240 and 290 nm, indicating the presence of ferric ion, decreased. By 3 h, the spectrum of ball-milled $FeCl_3$ solution almost matched with that of $FeCl_2$ solution, indicating that the ferric ions have been reduced. GC analysis confirms that the gas phase in the milling pot contained hydrogen gas, which may be generated according to the following reaction for the corrosion of iron by water.

$$3Fe + 4H_2O \rightarrow Fe_3O_4 + 4H_2 \quad (3)$$

This reaction occurs readily between iron and steam at high temperature; it does not normally occur at room temperature. However, the formation of single-phase Fe_3O_4 discussed earlier supports the idea that corrosion of the milling pot and balls by the mechanochemical effect is possible. These results imply that hydrogen gas generated during the ball-milling treatment can reduce part of the α-FeOOH to ferrous hydroxide ($Fe(OH)_2$) according to the

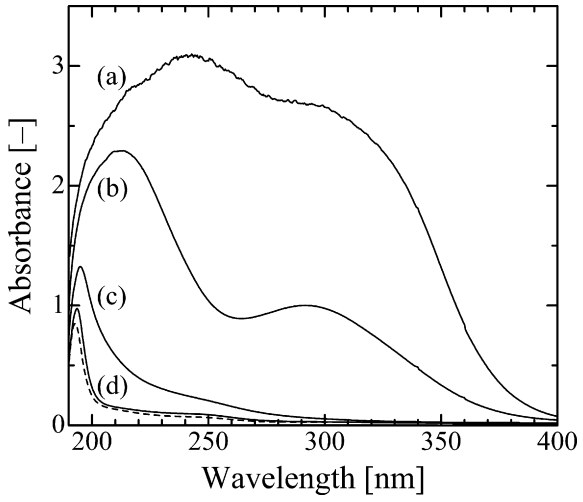

Fig. 6. UV spectra of $FeCl_3$ solutions (a) before milling and milled for (b) 1 h, (c) 2 h, and (d) 3 h. The broken line indicates the UV spectrum of unmilled $FeCl_2$ solution.

following reaction.

$$2\alpha\text{-FeOOH} + H_2 \rightarrow 2Fe(OH)_2 \quad (4)$$

Furthermore, the mechanochemical effect can promote formation of Fe_3O_4 nanoparticles according to the following reaction for the direct transformation of α-FeOOH to Fe_3O_4.

$$Fe(OH)_2 + 2\alpha\text{-FeOOH} \rightarrow Fe_3O_4 + 2H_2O \quad (5)$$

Details of the mechanochemical reaction mechanisms remain unknown and are a topic for further analysis.

4. Conclusions

Superparamagnetic Fe_3O_4 nanoparticles with a single crystal structure can be successfully synthesized from an aqueous α-FeOOH suspension at room temperature by the ball-milling treatment. The mechanochemical effect induced by this treatment causes reduction of ferric ions and promotes the formation and crystallization of Fe_3O_4 with neither additives (such as reducing agents, toxic organic solvents, or surfactants) nor heat. Thus, this method can be useful for development of environmentally friendly synthesis processes and for the functionalization of Fe_3O_4 nanoparticles by surface modification and particle compounding. A further benefit is that waste solutions containing ferric ion, such as plating waste and mine drainage, can be used as the initial solution.

References

[1] J. Huang, R. Zhao, H. Wang, W. Zhao, L. Ding, Biotechnol. Lett. 32 (2010) 817–821.
[2] Y. Cui, Y. Li, Y. Yang, X. Liu, L. Lei, L. Zhou, F. Pan, J. Biotechnol. (2010), doi:10.1016/j.jbiotec.2010.07.013.
[3] H. Kempe, M. Kempe, Biomaterials (2010), doi:10.1016/j.biomaterials.2010.07.107.
[4] K. Can, M. Ozmen, M. Ersoz, Colloids Surf. B 71 (2009) 154–159.
[5] J.-D. Qiu, H.-P. Peng, R.-P. Liang, X.-H. Xia, Biosens. Bioelectron. 25 (2010) 1447–1453.
[6] H. Fan, Z.-Q. Pan, H.-Y. Gu, Microchim. Acta 168 (2010) 239–244.
[7] Y.G. Li, H.S. Gao, W.L. Li, J.M. Xing, H.Z. Liu, Biores. Technol. 100 (2009) 5092–5096.
[8] P. Sun, H. Zhang, C. Liu, J. Fang, M. Wang, J. Chen, J. Zhang, C. Mao, S. Xu, Langmuir 26 (2010) 1278–1284.
[9] X. Dong, Y. Zheng, Y. Huang, X. Chen, X. Jing, Anal. Biochem. 405 (2010) 207–212.
[10] K. Hayashi, H. Ueno, R. Iino, H. Noji, Phys. Rev. Lett. 104 (2010) 218103.
[11] L. Zhou, J. Yuan, W. Yuan, M. Zhou, S. Wu, Z. Li, X. Xing, D. Shen, Mater. Lett. 63 (2009) 1567–1570.
[12] S. Guo, D. Li, L. Zhang, J. Li, E. Wang, Biomaterials 30 (2009) 1881–1889.
[13] J.E. Lee, N. Lee, H. Kim, J. Kim, S.H. Choi, J.H. Kim, T. Kim, I.C. Song, S.P. Park, W.K. Moon, T. Hyeon, J. Am. Chem. Soc. 132 (2010) 552–557.
[14] M. Mahmoudi, S. Sant, B. Wang, S. Laurent, T. Sen, Adv. Drug Deliv. Rev. (2010), doi:10.1016/j.addr.2010.05.006.
[15] C.M. Lee, H.J. Jeong, E.M. Kim, D.W. Kim, S.T. Lim, H.T. Kim, I.K. Park, Y.Y. Jeong, J.W. Kim, M.H. Sohn, Magn. Reson. Med. 62 (2009) 1440–1446.
[16] F. Hu, K.W. MacRenaris, E.A. Waters, E.A. Schultz-Sikma, A.L. Eckermann, T.J. Meade, Chem. Commun. 46 (2010) 73–75.
[17] Y. Zhang, J.-Y. Liu, S. Ma, Y.-J. Zhang, X. Zhao, X.-D. Zhang, Z.-D. Zhang, J. Mater. Sci. Mater. Med. 21 (2010) 1205–1210.
[18] C.Y. Haw, F. Mohamed, C.H. Chia, S. Radiman, S. Zakaria, N.M. Huang, H.N. Lim, Ceram. Int. 36 (2010) 1417–1422.
[19] E.M. Muzquiz-Ramos, D.A. Cortes-Hernandez, J. Escobedo-Bocardo, Mater. Lett. 64 (2010) 1117–1119.
[20] F. Gao, Y. Cai, J. Zhou, X. Xie, W. Ouyang, Y. Zhang, X. Wang, X. Zhang, X. Wang, L. Zhao, J. Tang, Nano Res. 3 (2010) 23–31.
[21] J. Qu, G. Liu, Y. Wang, R. Hong, Adv. Powder Technol. 21 (2010) 461–467.
[22] X. Hong, X. Chu, P. Zou, Y. Liu, G. Yang, Biosens. Bioelectron. 26 (2010) 918–922.
[23] Y. Shan, J.-J. Xu, H.-Y. Chen, Chem. Commun. 46 (2010) 4187–4189.
[24] S. Gustafsson, A. Fornara, K. Petersson, C. Johansson, M. Muhammed, E. Olsson, Cryst. Growth Des. 10 (2010) 2278–2284.
[25] T. Ozkaya, M.S. Toprak, A. Baykal, H. Kavas, Y. Köseoğlu, B. Aktaş, J. Alloys Compd. 472 (2009) 18–23.
[26] J.C. Aphesteguy, S.E. Jacobo, N.N. Schegoleva, G.V. Kurlyandskaya, J. Alloys Compd. 495 (2010) 509–512.
[27] R.A. Frimpong, J. Dou, M. Pechan, J.Z. Hilt, J. Magn. Magn. Mater. 322 (2010) 326–331.
[28] F. Yazdani, M. Edrissi, Mater. Sci. Eng. B 171 (2010) 86–89.
[29] T. Iwasaki, N. Mizutani, S. Watano, T. Yanagida, T. Kawai, J. Exp. Nanosci. 5 (2010) 251–262.
[30] N. Mizutani, T. Iwasaki, S. Watano, T. Yanagida, T. Kawai, Curr. Appl. Phys. 10 (2010) 801–806.
[31] X. Wen, J. Yang, B. He, Z. Gu, Curr. Appl. Phys. 8 (2008) 535–541.
[32] S. Yu, J. Wan, X. Yu, K. Chen, J. Phys. Chem. Solids 71 (2010) 412–415.
[33] J. Yan, S. Mo, J. Nie, W. Chen, X. Shen, J. Hu, G. Hao, H. Tong, Colloids Surf. A 340 (2009) 109–114.
[34] Y. Lai, W. Yin, J. Liu, R. Xi, J. Zhan, Nanoscale Res. Lett. 5 (2010) 302–307.
[35] W. Lu, Y. Shen, A. Xie, W. Zhang, J. Magn. Magn. Mater. 322 (2010) 1828–1833.
[36] T. Iwasaki, K. Kosaka, S. Watano, T. Yanagida, T. Kawai, Mater. Res. Bull. 45 (2010) 481–485.
[37] T. Iwasaki, K. Kosaka, N. Mizutani, S. Watano, T. Yanagida, H. Tanaka, T. Kawai, Mater. Lett. 62 (2008) 4155–4157.
[38] T. Iwasaki, K. Kosaka, T. Yabuuchi, S. Watano, T. Yanagida, T. Kawai, Adv. Powder Technol. 20 (2009) 521–528.
[39] Y. Ni, X. Ge, Z. Zhang, Q. Ye, Chem. Mater. 14 (2002) 1048–1052.
[40] R.C. O' Handley, Modern Magnetic Materials: Principles and Applications, Wiley-Interscience, New York, USA, 2000, p. 99.
[41] J. Lee, T. Isobe, M. Senna, Colloids Surf. A 109 (1996) 121–127.
[42] J.-H. Wu, S.P. Ko, H.-L. Liu, S. Kim, J.-S. Ju, Y.K. Kim, Mater. Lett. 61 (2007) 3124–3129.